RISET
Geologi dan Pertambangan

ACTIVE FAULT ZONES OF THE 2006 YOGYAKARTA EARTHQUAKE INFERRED FROM TILT DERIVATIVE ANALYSIS OF GRAVITY ANOMALIES

ZONA PATAHAN AKTIF GEMPA YOGYAKARTA 2006 BERDASARKAN ANALISIS TURUNAN KEMIRINGAN ANOMALI GAYABERAT

Lina Handayani

Pusat Penelitian Geoteknologi LIPI, Bandung

ABSTRACT The 2006 Yogyakarta Earthquake had caused a disaster in Bantul area. Several institutions had reported different results for the epicenter location. However, aftershocks studies indicated that the rupture area was at about 10 km east of Opak Fault. Analysis of gravity anomaly, including several degrees of residual anomalies and tilt derivative, facilitated this regional tectonic study to determine the structural constraints on the main earthquake and its aftershocks. The Yogyakarta area was primarily characterized by several SW-NE faults; one of them is the Opak Fault. Among those faults,, there are a series of WNW-ESE faults. Several groups of these lineations indicated a presence of some pairs of parallel strike-slips faults that formed pull-a-part basins. The obtained structural pattern has signified the dynamic response of the force from the subduction of the Australian Plate toward Sunda (Eurasia) Plate. The subduction force produced the strike-slip fault in a parallel direction of subduction, and subsequently, the faults caused the formation of thrust structures that are perpendicular to them.

Keywords: Yogyakarta 2006 earthquake, structural constraints, Opak Fault, gravity, residual anomaly, tilt derivative.

_____

_____

Lina Handayani
Pusat Penelitian Geoteknologi LIPI
Email : lina.handayani@gmail.com

ABSTRAK Gempabumi Yogyakarta pada tahun 2006 telah menyebabkan bencana di daerah Bantul dan sekitarnya. Lokasi episenter yang ditentukan oleh beberapa lembaga menunjukkan hasil yang berbeda. Tetapi analisa gempabumi susulan telah menunjukkan daerah pegerakan hingga 10 km ke sebelah timur dari Sesar Opak. Analisa anomali gayaberat yang terdiri dari perhitungan anomali sisa dan turunan kemiringan (tilt derivative) diharapkan dapat membantu studi tektonik regional dalam menentukan batasan struktur yang menyebabkan kejadian gempabumi di daerah Yogyakarta. Daerah ini dicirikan oleh sesar-sesar berarah BD (Barat daya)-TL (Timur laut), yang salah satunya adalah Sesar Opak. Di antara sesar-sesar tersebut, terdapat pula deretan sesar-sesar berarah BBL (Barat barat laut)-TTG (Timur tenggara). Beberapa kelompok kelurusan-kelurusan membentuk kemungkinan adanya cekungan pull-a-part, yang terbentuk karena adanya deretan sesar-sesar strike-slip. Pola struktur yang diperoleh menunjukkan respon dinamik dari subduksi Lempeng Australia terhadap Lempeng Eurasia (Sunda). Tekanan dari gaya subduksi menyebabkan terbentuknya sesar-sesar strike-slip. Kemudian sesar-sesar tersebut menyebabkan adanya struktur sesar naik yang tegak lurus terhadapnya.

Kata kunci: Gempabumi Yogyakarta 2006, batasan struktur, Sesar Opak, gayaberat, anomali sisa, turunan kemiringan.

INTRODUCTION

The Yogyakarta earthquake with a magnitude of 6.4 occurred early in the morning on 27 May 2006. The earliest report of NEIC (National

Earthquake Information Center) indicates that the epicenter of the shock was at the south coast of Yogyakarta Province, south of Opak River with a depth of 10 km. However, other institutions reported different locations of epicenters and focal mechanisms estimation. According to NIED (National Research Institute for Earth Science and Disaster Resilience - Japan), the epicenter was at the northeast end of the Opak Fault but, while the Harvard-CMT's result was at about 15 km east of the NEIC's result. All focal mechanisms indicated the right lateral strike-slip in NW-SE direction (Tsuji et al., 2009; Walter et al., 2008). The wide and noticeable differences in the epicenter locations, especially for this typical shallow event, caused difficulty in determining the related fault responsible to the event. Later, hundreds of aftershocks were recorded. Analysis from the aftershocks record suggested that the

location of the epicenter and its rupture was about 10 km east of that earlier report (Bantul) (Sulaeman et al., 2008; Walter et al., 2008).

A 2D resistivity model from a magnetotelluric survey crossing the Opak Fault indicated a low anomaly body dip to the east. Even though the location is not precisely at the Opak Fault, it might represent the fault plane responsible for the earthquake (Grandis et al., 2006). A gravity study of the region had plotted the faults distribution based on the residual gravity anomaly (Widijono and Setyanta, 2007). However, the map could not explain the structures that might be responsible for the aftershocks. Nevertheless, the 2006 Yogyakarta Earthquake was then assumed as an activation of a fault, whether it was the Opak Fault or another older fault at its east as suggested by (Setijadji et al., 2007).
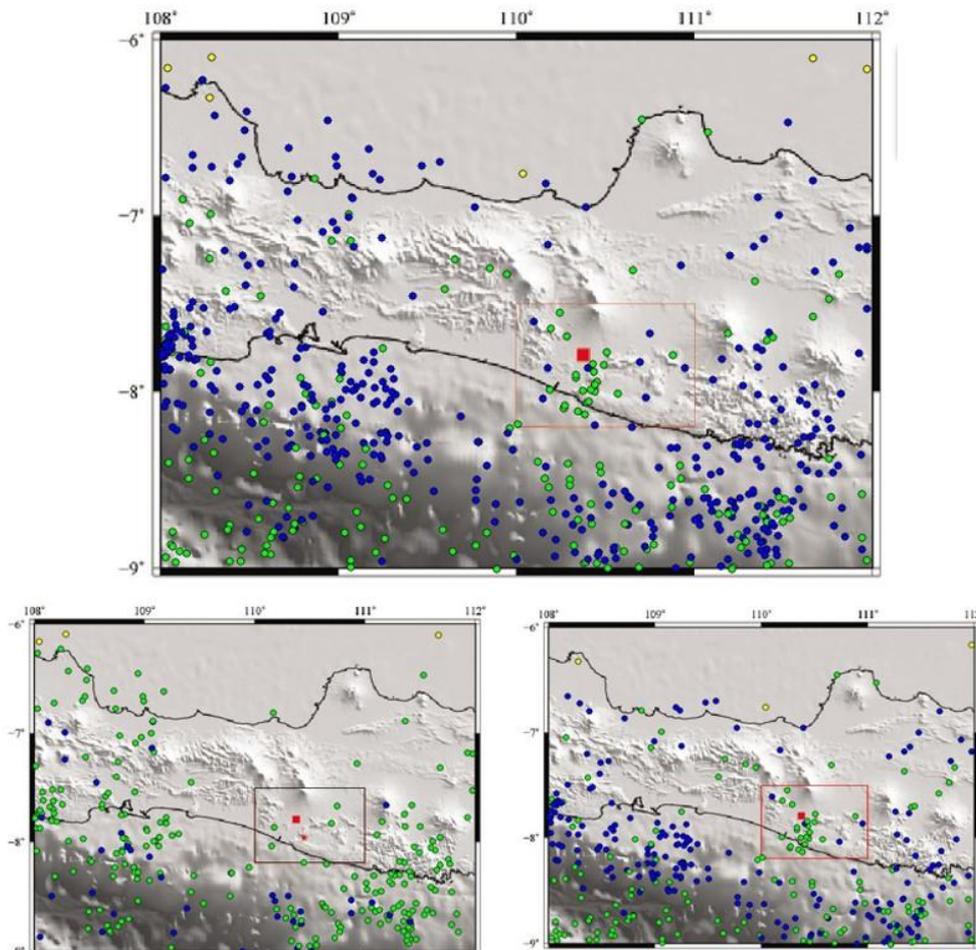

Figure 1. Epicenters distribution of events since 1971 to 2018, green circles for shallow events (< 60 km depth) and blue circles for intermediate depth events (60 – 300 km) (source: NEIC-USGS). The solid red square is the Yogyakarta City. Almost all shallow events in Yogyakarta region (green circles in the red border box) occurred after May 27, 2006. Left: events before May 2006 since 1971. Right: events after May 2006 – 2018.

In general, the fault activities indicated more complex structures at the southern part of Java Island. The force that might affecst the formation of the structures at this area is mostly from the subduction of the Indo-Australian Plate toward the Eurasian Plate. All informations on this Yogyakarta earthquake and its aftershocks inspired a renewed question on the tectonics of Yogyakarta area. Understanding the activity system of the faults, of any ages, for possible future earthquakes are very important. A detail probabilistic seismic hazard analysis required precise information on the main trigger of the earthquakes. Therefore a thorough examination of the fault that caused the Yogyakarta earthquake and its aftershocks need to be resolved for future mitigation works. In this work, we reanalyzed the gravity data by some edge detecting techniques and compared the result to the published aftershocks studies. Our result included the distribution of structural lines derived from gravity data, which might contribute to the main and aftershocks events of Yogyakarta 2006 earthquakes.

REGIONAL GEOLOGY

Yogyakarta is located at the southern part of Central Java that was substantially controlled by the subduction of Indo-Australian Oceanic Plate towards the Eurasian Continental Plate. The subduction activity was not only resulted in earthquakes and tsunamis but also the formation of volcanoes along the south of Java Island. Merapi Volcano is one of the most active volcanoes in the world and has a significant impact on the geological – morphological condition nearby. Yogyakarta is located at an almost flat region bordered by high terrains at its east and west (Figure 1) The coast at the south of Yogyakarta valley is a gentle slope beach that is open to the Indian Ocean. The coasts at the east part of the province are mostly steep due to the hilly morphology of the Southern Mountain.

Province of Yogyakarta was known as the province at the foot of Merapi Volcano. Yogyakarta city itself is located in the middle of Bantul Graben that was filled by the young volcanic deposit of Merapi Volcano. The graben/valley is bounded by an andesitic breccia – lava flow dome at the west and carbonaceous-volcanic rocks hills at the east. Bantul graben (valley) is bordered by the Opak Fault (River) at the east and Progo River at the west (Figure 1). The structural trend of the area is NE-SW. Limestone and karst landscape of Miocene
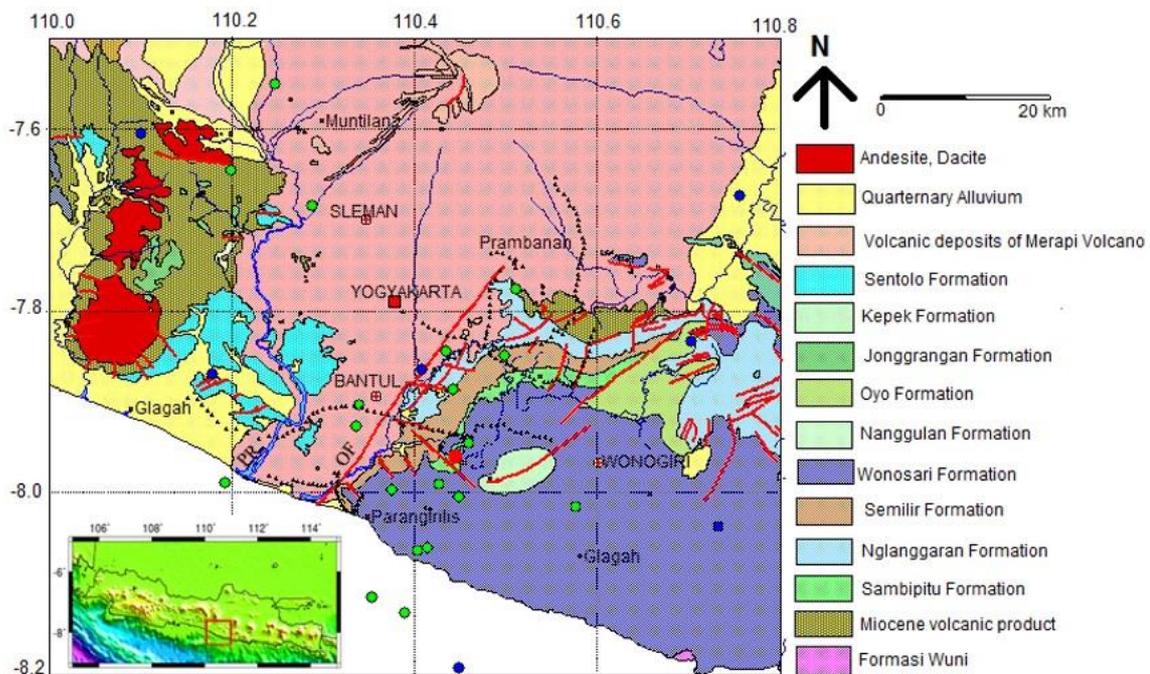

Figure 2. Geological map of Yogyakarta. Red lines are structures (lineations) (Rahardjo et al., 1995). Green and blue circles are epicenters of past earthquake events, for shallow and intermediate depths, respectively (source: NEIC-USGS). PR = Progo River, OF = Opak Fault.

Wonosari Formation characterized the geological condition of the eastern part of the Yogyakarta region (Karnawati et al., 2006). Between the wide karst topography and the Bantul Graben, there are several Miocene formations: Semilir, Nglanggaran, and Sambipitu Formations. Semilir and Nglanggaran formations mostly consist of older volcanic deposits, while Sambipitu Formation contains mostly sedimentary rocks (sandstone and conglomerate) (Rahardjo et al., 1995).

The dome at the west of the Bantul graben is the Kulon Progo Mountain, which has Miocene andesite in the center. According to (Syafri et al., 2013), this andesite hill is in accord with the regional tectonic pattern. As in the eastern of the basin, there is also a limestone landscape (Sentolo and Jonggrangan Formation). Older volcanic deposits are also represented by Kebobutak and Bemellen Formations. The oldest sandstone intercalates by lignite, claystone, and limestone formed the Nanggulan Formation (Rahardjo et al., 1995).

AFTERSHOCKS SEISMICITY

Earthquake activity of this part of Java is relatively low compared to other regions in front of the Java Subduction Zone. Figure 1 shows the epicenter distribution of several events ever recorded. All events in green had a depth less than 60 km, and the blue ones had a depth of more than 60 km. The deep and offshore events were directly caused by the seismogenic zone within the subducted slab. The shallow events that appear to be sporadically distributed on land might indicate faults activities. There were more events offshore than in land. Those offshore events were mostly studied in the past due to their vast amount of events. The earthquake on May 26, 2006, had reminded us of the importance of in-land events. There were at least four epicenter location results from four institutions for this earthquake (Kawazoe and Koketsu, 2010). The extent of differences (more than 10 km in the distance) between the locations caused variation in analysis results in finding the fault that responsible to the event. However, the aftershocks data had limited the possible active zones.

The earliest aftershocks relocation study has indicated the three clusters of events (blue shaded area in Figure 2) (Anggraini et al., 2011). The first cluster was about 10 km east of Opak Fault, with SW-NE trend parallel to the fault. The
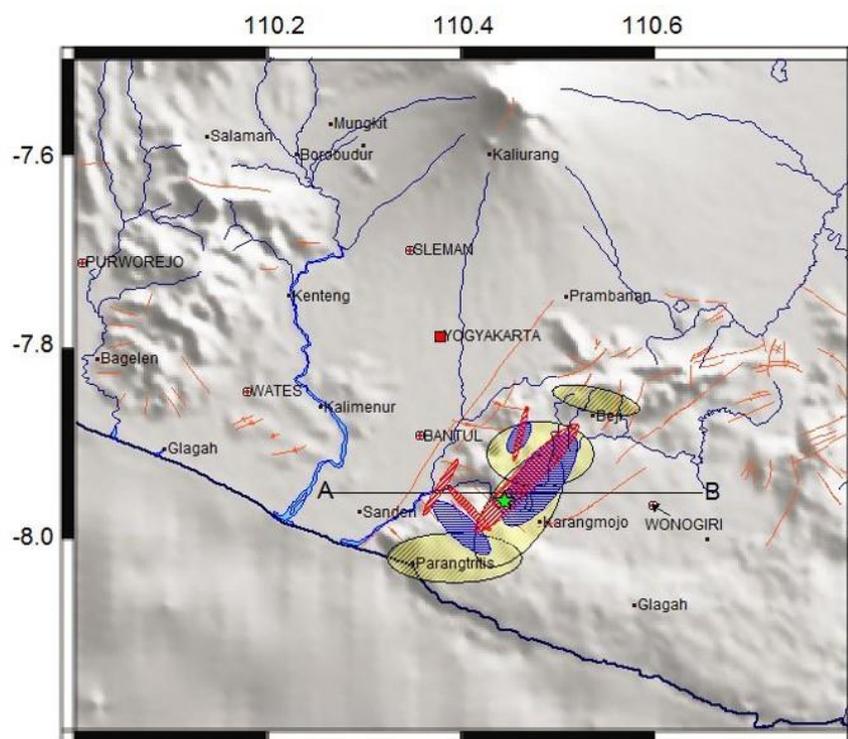

Figure 3. Review of aftershocks studies. The green star is the location of the 2006 main shock event according to USGS. Blue shaded areas are the region of aftershocks events from Anggraini et al. (2011) and Walter et al. (2008). Red shaded areas are from Wulandari et al. (2018). Yellow shaded areas are from Husni et al. (2018).

second cluster was the one perpendicular to the Opak fault, from the southernmost of the first cluster to the northwest direction. The third cluster was located closer to the Opak River and paralleled to the first cluster. The last cluster has a relatively shallower depth (3-6 km) than others (Anggraini et al., 2011; Walter et al., 2008). Recent studies of aftershocks had plotted more aftershock events in the area from the Opak Fault lineation to 10 – 15 km east with depth less than 20 km (yellow shaded area in Figure 2)(Diambama et al., 2018; Husni et al., 2018). Their seismic profiles indicated a dipping east reverse fault. Further study of the aftershocks relocation data showed an N42°E fault strike with 80° dip parallel to Opak River (red shaded area in Figure 2) (Wulandari et al., 2018). The aftershocks are distributed in the circumference of the USGS version of the mainshock hypocenter. Therefore, these most recent result of the aftershocks analysis (Husni et al., 2018; Walter et al., 2008; Wulandari et al., 2018) had confirmed the fault activity at the east of Opak River.

Even earlier, based on the earliest aftershocks study, Kawazoe and Koketsu (Kawazoe and Koketsu, 2010) mentioned the two different events in two fault segments: near hypocenter and at its southwest. Setijadji et al. (2007) suggested an unnamed strike-slip fault with NNE-SSW trend, parallel to Opak Fault, and believed to have existed since Plio-Pleistocene. The aftershocks events distributed within the areas covered by Tertiary sedimentation of Nglanggaran, Semilir and Sambipitu Formations, between karst topography of Wonosari Formation and young volcanic deposit of Bantul graben.

The depth of the events that mainly at 10-15 km are tightly clustered within 10 km east of Opak Fault (Husni et al., 2018). The rest of events spreads loosely from the surface to the cluster's center with the approximate dip of 45°, in both west and east direction. A group at the west might be connected to the Opak Fault surface line. As stated before, the 2006 main earthquake itself has a strike-slip motion with a relatively small dip (USGS). The aftershocks distribution might indicate that the main shocks (in the middle of the cluster) ruptured the area, and propagated along all weak zones. Those weak zones are all the smaller faults of the area. And this

propagation of the rupture had been still active to at least in 2017 when the last event was recorded.

METHODS

Gravity anomaly was obtained from the regional Bouguer anomaly data from (Untung and Sato, 1978) added by a few direct measurements that were executed soon after the 2006 earthquake occurred. The last measurement data only covered a few locations within the Bantul area, which experienced high damages (small black points in Figure 2). However, since the gravity method is one of the geophysics instruments for studying the regional area, we should combine them with the available regional data. The acquired gravity data were processed and corrected with similar methods to obtain the previous regional Bouguer anomaly (Untung and Sato, 1978).

Data enhancement techniques such as regional trend filtering and other derivative based filtering have been applied for the analysis of the gravity field. We used the least square polynomial concept to separate the regional trend from the sources, which are the basement configurations in this case (Lowrie, 2007). The total regional values of gravity anomalies are

$$\Delta g_g = \Delta g_o + \Delta g_1 x + \Delta g_2 x^2 + \Delta g_3 x^3 + ... + \Delta g_x x^x \text{...(1)}$$

where Δg_1, Δg_2, and Δg_3 are the regional values for first, second, and third order respectively.

One of many filtering methods to detect the main geological structures is the tilt derivative method (TDR). The TDR is one of the edge detection techniques for gravity and magnetic data. Actually, the exact correlation between the lineaments of potential data and the faults/folds/structural pattern was not well (Blakely, 1995; Hinze et al., 2013). However, the patterns would certainly help determining the structural pattern qualitatively (Ghosh, 2016; Nasuti et al., 2012). The tilt derivative is the angle between the total horizontal derivative (x and y directions) and the first vertical derivative:

$$TDR = \tan^{-1}\left(\frac{VDR}{THDR}\right) \text{radian ....(2)}$$

where *VDR* is the first vertical derivative and *THDR* is the total horizontal derivative of the potential field (Nasuti et al., 2012; Verduzco et al., 2004). The horizontal derivative is a measure

of the change (gradient) of the anomaly in the x and y direction. This derivative involves a phase transformation that might produce anomaly peaks or troughs about the sources edges of wide bodies. A vertical derivative is the rate of change of the potential with depth. It is a zero phase filter, which will not affect the anomaly peaks but will sharpen the anomaly (Saad, 2006). Verduzco et al. (2004) used the total horizontal derivative of TDR (THTDR) for further edge detector

$$THTDR = \sqrt{\left(\frac{\partial TDR}{\partial x}\right)^2 + \left(\frac{\partial TDR}{\partial y}\right)^2} \quad radian/km$$
………………………..(3)

The technique of detecting the edges of anomalous sources has been proven in synthetic modeling (Saad, 2006; Saada, 2016; Verduzco et al., 2004). We applied all filtering calculation using the Oasis Montaj software.

RESULT AND DISCUSSION

Bouguer gravity anomaly distribution was presented on the map at Figure 4a. High anomalies appear in two regions: at a mountain region near Bagelen (Kulon Progo), and the south coast about Parangtritis (about the south end of Opak Fault). Low anomalies mostly are at the northernmost of the study area. The regional average gravity anomaly is at the range of 50 to 100 mgal. Surprisingly, the flat regions of Yogyakarta Valley to the south (coast), the vast region at the east of Yogyakarta, and the high hills in between have a similar range of anomalies (green area, anomaly about 80 mgal). The high anomaly areas are coincidently located at the Miocene karst formation of Wonosari (red zone at the east), and Miocene andesite mountain of Kulon Progo (red zone at the west). The lowest gravity anomaly was at the north (Kaliurang), at the active volcanic region.

The residual anomaly maps might present the basement configuration (Figure 4b, 4c, 4d). There are at least two major trends of anomalies in these maps: the west-east trends and the southwest-northeast trends; both separate the high and low anomalies area. The first residual map (Figure 4b) showed the west-east trend high anomalies (red-pink) at the north of the latitude line of 7.8°S. The high anomaly region, which extended from west to east, is mostly associated

with the igneous rock layer near or on the surface. The east-west structure at about this 7.8°S line separated the high anomaly at the north to the south region. At the south, the low anomaly closure appeared in Bantul area to the south coast (blue). The closure in Bantul area has the southwest-northeast trend. The Bantul Basin is more likely established from a-pull-a-part graben due to the movement of the pair of SW-NE structures and most destroyed area during the 2006 Yogyakarta earthquake.

In the second residual map (Figure 4c), the high anomalies were in the same region as the previous order. Nevertheless, the low anomalies were extended to the east, covering the area of Beji and Wonogiri (Wonosari Basin), in E-W direction. The E-W low anomaly might consist of at least two sub-clusters: Beji and Wonogiri, which are relatively small. All of the low anomaly clusters are separated by NE-SW faults and likely had a-pull-a-part graben origin.

The high residual anomalies area in the third residual map was separated by average anomalies between Yogyakarta and Prambanan (Figure 4d). However, the prominent high anomalies appeared in Parangtritis (south coast). As for the low anomaly, it was thinning in Bantul Basin but widening and stronger in Beji-Wonogiri (Wonosari Basin).

In short, most of the regions south of 7.8°S have deep basements that formed basins, except a small area at the south (Parangtritis). The low anomaly closures might represent the existence of basins. The Bantul Basin should be deeper since it appeared at the first residual map. On the surface, this region is also known as the Bantul Basin or valley, which is covered by young volcanic deposit from Merapi. The Wonosari Basin should be shallower due to the presence of low anomaly at the third residual anomaly. However, the area has hilly morphology and is covered by older deposition of Miocene formations. The deposition includes the limestone of Wonosari limestone, and other sediments and volcanic products of Miocene age (Semilir, Nglanggaran, and Sambipitu Formations). All basins are separated by several parallel NE-SW faults at the south of the E-W extended fault at 7.8°S.

(a) Bouguer Anomaly

(b) First Order Residual Anomaly

(c) Second Order Residual Anomaly
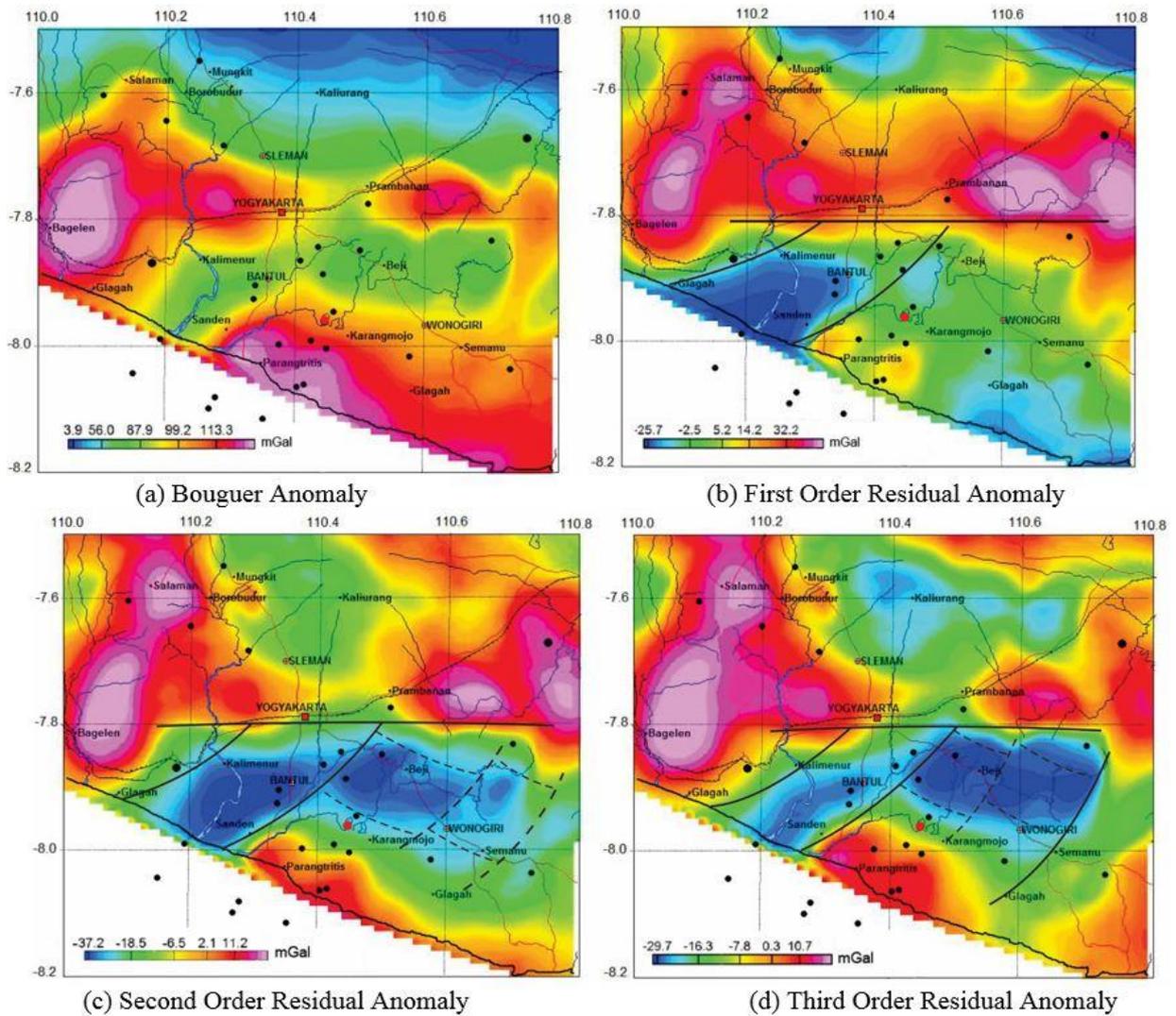
(d) Third Order Residual Anomaly

Figure 4. Gravity anomaly of Yogyakarta region.

More filtering techniques were expected to provide better structures lineation. Here we have the tilt derivative of the anomaly (TDR), and the total horizontal derivative of that tilt derivative (THTDR) (Figure 5). The TDR map (5a) showed an almost identical pattern to the second residual anomaly map, with west-east high anomalies area was at the north of the 7.8°S and low anomalies in Bantul and Beji-Wonogiri areas. However, there were more small anomaly patterns in the area around Parangtritis – Karangmojo – Wonogiri – Semanu – Glagah that did not appear in the residual anomaly. The tilt derivative or tilt angle value of zero was the one we would associate to the edges of structures or bodies. Therefore, we could draw more edges (lineations) based on this TDR map.

Those edges were better signified in the total horizontal derivative of the tilt angle map and marked by the dashed lines (Figure 5b). A circular pattern on the west represents the edges of the andesitic hill

(Kulon Progo). In the middle, Opak Fault was located right on one of the lineation patterns. The horizontal east-west patterns, at the east of Opak Fault, were already drawn as faults in the previous geological map (Rahardjo et al., 1995). Based on those indications, we drew more structural lineations based on the map of THTDR. East-West trending patterns dominated the northern area (north of -7.80 line). However, we concentrated the discussion to the south of that line, where aftershock events occurred.

7

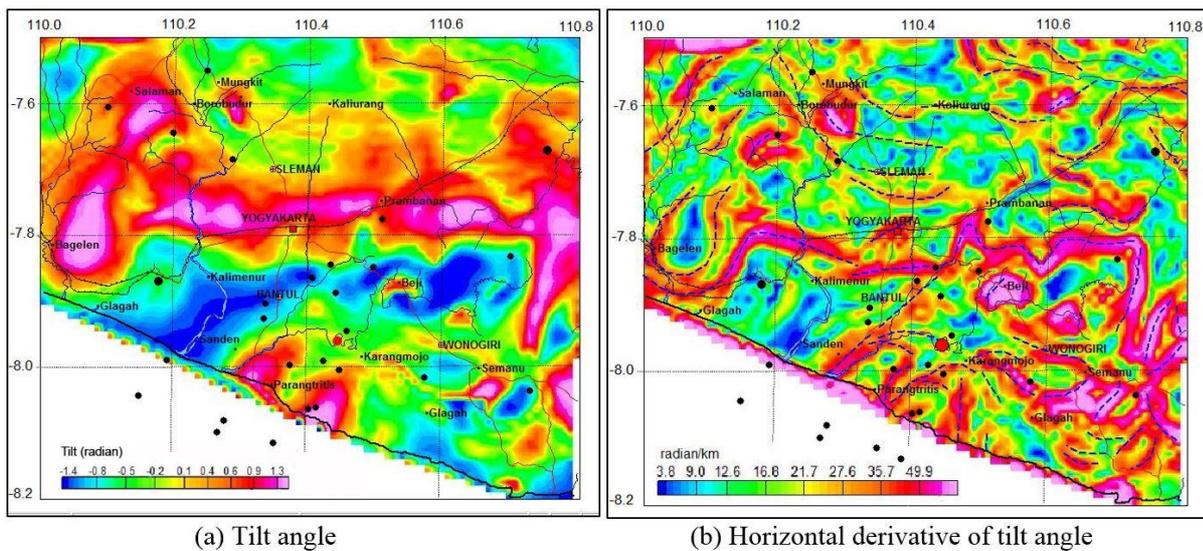(a) Tilt angle   (b) Horizontal derivative of tilt angle

Figure 5. (a) Tilt angle (TDR) of the Bouguer gravity anomaly. (b) Total horizontal derivative of the tilt derivative (THTDR) of the Bouguer anomaly. Black dash lines are lineations based on both derivatives, red dot is the epicentre of the 2006 main earthquake, and black dots are the epicenters of earthquake events.

Interpretation of the THTDR and the topographical analysis were depicted in Figure 6. There were two trends of structures: west-east and southwest–northeast. Several SW-NE parallel lineations from the coast to the northeast with the length of about 30 – 40 km could be associated with the topographical trend (Figure 6). The main result of these structures was the Bantul Basin that is formed between two extended SW-NE faults. Added by the E-W structural trend at its east, forming the other basins (Beji – Wonogiri). These eastern and smaller basins were possibly established in earlier times, since depositions in this area belong to older formations (mostly Miocene volcanic deposits). However, the depth of the basin is shallower. There should be different in origin or in force of tectonic activities that developed these basins.

Secluded from its surrounding, Parangtritis area has a high anomaly, and the THTDR also indicated edges around the area. Besides, the TDR edges also presented several short fault lineations that might be related to paleo-landslides as suggested by previous research (Husein et al., 2010). The area is a part of Wonosari Karst topography, but it has Nglanggaran Formation of andesitic breccia as the basement.

The development of geological structures is undoubtedly controlled by regional tectonics. The structural patterns as shown in Figure 6 confirmed the significant control of the subduction movement of the Indian-Australian plate toward the Sundaland. The different lineation distributions indicated several parallel SW-NE trending faults and WNW-ESE trending shorter faults. The SW-NE faults, which are perpendicular to the trench, are most likely strike-slip faults with thrust components. The profiles from aftershocks study (Husni et al., 2018) and magnetotelluric survey (Grandis et al., 2006) had indicated the thrust fault characteristic
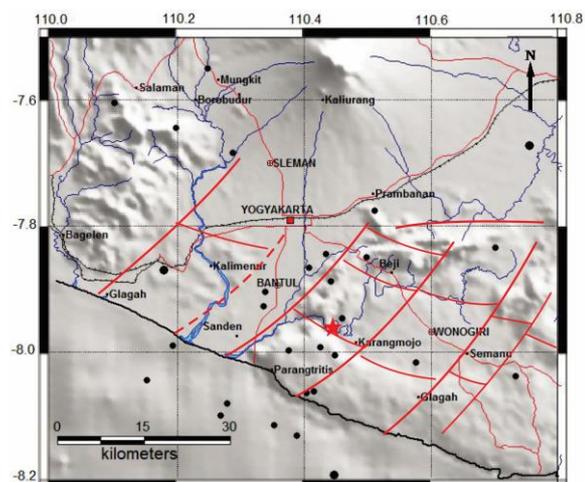

Figure 6. Lineation distribution based on the analysis of the tilt angle and its total horizontal derivative on the topography map. Red star is the main earthquake on May 27, 2006, and black dots are the recorded earthquake events.

of Opak Fault. This thrust property might be applied to the other SW-NE lineation since the aftershocks relocation study had indicated that most events occurred along another fault about 15 km at the east of and parallel to Opak Fault.

Another cluster of aftershock events occurred in the southern part and formed the WNW-ESE lineation. In oblique subduction cases, strike-slip faults accommodate the trench-parallel components of oblique subduction. For instances, the Sumatra Fault Zone along the Java-Sumatra Trench, the Median Tectonic Line of Southwestern Japan along Nankai Trough, and the Philippine Fault System along Philippine Trench (Noda, 2013). Those strike-slips are typically long but occasionally segmented. The subduction zone at the south of Java is not as oblique as Sumatra. Nevertheless, there are small trench components that might generate shorts strike-slips faults that parallel to the trench.

CONCLUSION

The epicenters of the Yogyakarta earthquake and its aftershocks were distributed in the southeast of the Yogyakarta, from about the location of Opak Fault to the east. The spreading of the events drew the attention to the active structures of this area. Gravity data were applied for this purpose since the regional gravity data was ready and available. The gravity analysis is also excellent in mapping the pattern of the regional geological structures. Based on the Bouguer Anomaly map, we derived several derivatives. The first, second, and third order of residuals had indicated typical low gravity anomaly at the Bantul and Beji-Wonogiri, which represented two basins. These two basins might differ in the age of origin and depth. The Bantul Basin is mostly covered by recent volcanic deposit from Merapi, and the Beji-Wonogiri Basin filled by older sediments (Miocene). The edge detection from gravity anomaly derivatives had indicated the structural pattern of South Yogyakarta area. The outlines at the west and north of Beji-Wonogiri Basin could be confirmed by the structures from current geological map. However, the complex edges (lineations) in the region of Wonosari Formation need further geological validation. On the other hand, these edges are located within the area of the earthquakes distribution. Hence, confirmed the existence of the active structures at the east of Opak Fault.

REFERENCES

Abidin, H. Z., Andreas, H., Kato, T., Ito, T., Meilano, I., Kimata, F., Natawidjaya, D. H., Harjono, H., 2009. Crustal deformation studies in Java (INDONESIA) USING GPS. J. Earthq. Tsunami 3, 77–88.

Anggraini, A., Sobiesiak, M., Walter, T. R., Luehr, B. G., 2011. The 26 May 2006 Yogyakarta Earthquake: Its aftershocks and Its Relation Towards the Regional Seismotectonic Setting, in: American Geophysical Union Fall Meeting. p. T14A–05.

Blakely, R. J., 1995. Potential Theory in Gravity and Magnetic Applications. Cambridge University Press, Cambridge, UK. DOI:10.1017/CBO9780511549816

Chingtham, P., Chingtham, P., Sharma, B., Chopra, S., SinghaRoy, P., 2016. Statistical analysis of aftershock sequences related with two major Nepal earthquakes: April 25, 2015, MW 7.8, and May 12, 2015, MW 7.2. Ann. Geophys. 59, S0540. DOI:10.4401/ag-7025

Diambama, D., Anggraini, A., Nukman, M., Luehr, B. G., Suryanto, Wiwit, 2018. Velocity Structure around the 2006 M6.3 Yogyakarta Earthquake Zone Inferred from Seismic Tomography, in: 20th EGU General Assembly, EGU 2018. p. 2156.

Ghosh, G. K., 2016. Interpretation of Gravity Data using 3D Euler Deconvolution, Tilt Angle, Horizontal Tilt Angle and Source Edge Approximation of the North-West Himalaya. Acta Geophys. 64, 1112–1138. DOI:10.1515/acgeo-2016-0042

Grandis, H., Nurhasan, N., Widarto, D. S., Mogi, T., 2006. Importance of Geophysical

Investigations of Active Faults and Crustal Structures in Earthquake Hazard Mitigation, in: International Workshop on Integration of Geophysical Parameter as a Set of Large Earthquake Precursors,. BMG - LIPI - ITB.

Hinze, W. J., von Frese, R. R. B., Saad, A. H., 2013. Gravity and Magnetic Exploration, 1st ed. Cambridge University Press, Cambridge, UK. DOI: 10.1017/CBO9780511843129

Husein, S., Sudarno, I., Pramumijoyo, S., Karnawati, D., 2010. Paleostress Analysis To Interpret the Landslide Mechanism: a Case Study in Parangtritis, Yogyakarta. J. Southeast Asian Appl. Geol. 2, 104–109. DOI:10.13140/RG.2.1.2325.3200

Husni, Y. M., Nugraha, A. D., Rosalia, S., Zulfakriza, Sahara, D. P., 2018. Aftershock location determination of the 27 May 2006, M 6.4 Yogyakarta earthquake using a non-linear algorithm: A preliminary results, in: AIP Conference Proceedings 1987. p. 020049. DOI:10.1063/1.5047334

Karnawati, D., Pramumijoyo, S., Hendrayana, H., 2006. Geology of Yogyakarta , Java :, in: IAEG2006 Proceeding,. The Geological Society of London, pp. 1–7.

Kawazoe, Y., Koketsu, K., 2010. Source Fault and RUpture Process of the 2006 Yogyakarta Earthquake, in: American Geophysical Union, Fall Meeting. p. S43A–2030.

Lowrie, W., 2007. Fundamentals of Geophysics, second edition. Cambridge University Press, Cambridge, UK. DOI:10.1017/CBO9780511807107

Nasuti, A., Pascal, C., Ebbing, J., 2012. Onshore-offshore potential field analysis of the Møre-Trøndelag Fault Complex and adjacent structures of Mid Norway. Tectonophysics 518–521, 17–28. DOI:10.1016/j.tecto.2011.11.003

Noda, A., 2013. Strike-Slip Basin – Its Configuration and Sedimentary Facies, in: Itoh, Y. (Ed.), Mechanism of Sedimentary Basin Formation. Intech, pp. 27–57. DOI:10.5772/56593 47

Ogata, Y., Tsuruoka, H., 2016. Statistical monitoring of aftershock sequences: A case study of the 2015 Mw7.8 Gorkha, Nepal, earthquake the 2015 Gorkha, Nepal, Earthquake and Himalayan Studies: First Results 4. Seismology. Earth, Planets Sp. 68. DOI:10.1186/s40623-016-0410-8

Rahardjo, W., Sukandarrumidi, Rosidi, H. M. D., 1995. Geological Map of the Yogyakarta Quadrangle, Java. Geological Survey of Indonesia.

Saad, A. H., 2006. Understanding gravity gradients—a tutorial. Lead. Edge 25, 942–949. DOI:10.1190/1.2335167

Saada, S. A., 2016. Edge detection and depth estimation of Galala El Bahariya Plateau, Eastern Desert-Egypt, from aeromagnetic data. Geomech. Geophys. Geo-Energy Geo-Resources 2, 25–41. DOI:10.1007/s40948-015-0019-6

Setijadji, A. L. D., Fukuoka, B. K., Ehara, C. S., 2007. Geology of Yogyakarta earthquakes 2006 (central Java , Indonesia): Current understanding based on integration of research outputs in geology , geophysics and remote sensing . 9, 9–10.

Sulaeman, C., Dewi, L. C., Triyoso, W., 2008. Karakterisasi sumber gempa Yogyakarta 2006 berdasarkan data GPS. J. Geol. Indones. 3, 49–56.

Syafri, I., Budiadi, E., Sudradjat, A., 2013. Geotectonic Configuration of Kulon Progo Area , Yogyakarta Konfigurasi Tektonik Daerah Kulon Progo , Yogyakarta. Indones. J. Geol. 8, 185–190.

Tsuji, T., Yamamoto, K., Matsuoka, T., Yamada, Y., Onishi, K., Bahar, A., Meilano, I., Abidin, H. Z., 2009. Earthquake fault of the 26 May 2006 Yogyakarta earthquake observed by SAR interferometry. Earth, Planets Sp. 61, e29–e32. DOI:10.1186/BF03353189

Untung, M., Sato, Y., 1978. Gravity and geological studies in Jawa, Indonesia, Spesial Pu. ed. Direktorat Geologi, Indonesia, Bandung.

Utsu, T., 1970. Aftershocks and Earthquake Statistics (I). J. Fac. Sci. Geophys. 3, 129–195.

Verduzco, B., Fairhead, J. D., MacKenzie, C., 2004. New insights into magnetic derivatives for structural mapping. Lead. Edge 23, 116–119.

Walter, T. R., Wang, R., Luehr, B. G., Wassermann, J., Behr, Y., Parolai, S., Anggraini, A., Günther, E., Sobiesiak, M., Grosser, H., Wetzel, H. U., Milkereit, C., Sri Brotopuspito, P. J. K., Harjadi, P., Zschau, J., 2008. The 26 May 2006 magnitude 6.4 Yogyakarta earthquake south of Mt. Merapi volcano: Did lahar deposits amplify ground shaking and thus lead to the disaster? Geochemistry, Geophys. Geosystems 9, 1–9. DOI:10.1029/2007GC001810

Widijono, B. S., Setyanta, B., 2007. Anomali gaya berat, kegempaan serta kelurusan struktur geologi daerah Yogyakarta dan sekitarnya. J. Sumber Daya Geol. 17, 74–90.

Wulandari, A., Anggraini, A., Suryanto, W., 2018. Hypocenter Analysis of Aftershocks Data of the Mw 6.3, 27 May 2006 Yogyakarta Earthquake Using Oct-Tree Importance Sampling Method. Appl. Mech. Mater. 881, 89–97. DOI:10.4028/www.scientific.net/AMM.881.89